Variation of Rock Electrical Resistivity in Andesitic-Trachytic Volcanic Geothermal Areas. A Case Study of Lili-Sepporaki, Sulawesi island- Indonesia

Mutebi, Denis
Faculty of Geological Engineering, Universitas Padjadjaran

Andi Agus Nur
Faculty of Geological Engineering, Universitas Padjadjaran

Agus Didit Haryanto
Faculty of Geological Engineering, Universitas Padjadjaran

Wiwid, Joni
Centre for Minerals, Coal, and Geothermal Resources (PSDMBP)

https://doi.org/10.5109/4068609

出版情報：Evergreen. 7 (3), pp.314-322, 2020-09. 九州大学グリーンテクノロジー研究教育センター
バージョン：

Variation of Rock Electrical Resistivity in Andesitic-Trachytic Volcanic Geothermal Areas. A Case Study of Lili-Sepporaki, Sulawesi island- Indonesia

Denis Mutebi[1,*], Andi Agus Nur[1], Agus Didit Haryanto[1], Joni Wiwid[2]

[1]Faculty of Geological Engineering, Universitas Padjadjaran, Indonesia.

[2]Centre for Minerals, Coal, and Geothermal Resources (PSDMBP), Indonesia.

*Author to whom correspondence should be addressed:

E-mail: denis2003mutebi@gmail.com

(Received March 4, 2020; Revised July 27, 2020; accepted August 24, 2020)

Abstract: The objective of this paper is to investigate how electrical resistivity changes as electromagnetic waves penetrate deep into the subsurface of Lili-Sepporaki geothermal prospect, using Magnetotelluric data. Lili Sepporaki is an andesitic-trachytic volcanic-rich area located in western Sulawesi-Indonesia. Magnetotelluric data was processed using SSMT2000 and MTEditor software programmes. Results show that resistivity of rocks generally increases with decreasing frequency, that is; less than 100 Ohm-m for frequencies greater than 100 Hertz; and fluctuates between 100 -1000 Ohm-m for frequency range 1- 0.1 Hertz. Resistivity also increases with depth of penetration of electromagnetic waves. Weathering, hydrothermal alteration, and many times fluids increase the conductivity of rocks. A low resistivity anomaly is seen around the hot spring, northwards. Presence of fluids in an intensively fractured volcanic rock lowers its resistivity. In the future, another Magnetotelluric sounding should be carried with much more measurement stations followed by a three-dimensions interpretation.

Key words: Magnetotelluric, electromagnetic, SSMT2000, MTEditor, alteration.

1. Introduction

Indonesia has an abundance of geothermal energy sources, which are spread along a volcanic path on the "Ring of fire" [1-2]. Increasing threat posed by global warming and climate change has drawn the attention of global researchers and decision makers to renewable energy, contextually geothermal energy, as potential remedy [3]. Contrary, Indonesia heavily relies on non-renewable energy such as oil and coal, as its key energy source [4]. Renewable energy, the opposite of non-renewable energy, basically refers to energy resources that always exist and produce no greenhouse gases such as Carbon dioxide [5]; thus more efforts should be put in renewable energy utilization in Indonesia [6-7].

Lili Sepporaki is a geothermal prospect located in Polewali Mandar district, Western Sulawesi-Indonesia. Indonesia is strategically situated at the confluence of three tectonic namely; Pacific, Eurasia and Indo-Australian. The context of plate tectonism provides extensive but worthwhile clues about the geothermal prospect regions. The only thermal manifestations in this prospect are the hot springs and altered rocks. The hot springs' have a water temperature of 97°C, Chloride water and neutral pH water; the reservoir temperature is approximated to be 190°C [8] and the geothermal system is allegedly driven by heat from plutonic activity.

Electrical resistivity methods such as magnetotellurics have been always successfully deployed in geothermal exploration. Magnetotellurics (MT) techniques has been fruitfully used in Taupo volcanic zone (TVZ) in New Zealand and found a low resistivity below 600m depth which is linked to a fractured and intensely hydrothermally altered layer of rhyolite and tuffs, owing to the borehole in the vicinity [9]. Change in electrical resistivity of the rock-fluid volume is the most important physical property change due to the presence of a hydrothermal system, other than elevated temperature and heat flow[10]. Ionic conduction in rocks increases with increased porosity, increased salinity and increased amounts of certain minerals such as clays. Hydrothermal systems, which are generally characterized by one or more of these features, are therefore associated with a low-resistivity anomaly [11]. Near the surface, a reduction in resistivity can be attributed to hydrothermal alteration of

rocks into smectite clays (conductive) and the existence of very hot, briny fluid. However, at a higher depth, an elevation in resistivity may be due to a decrease in porosity and a shift of the alteration product to less conductive clays such as illite and chlorite[12].

The objective of this paper is to investigate the variation of resistivity with frequency in andesitic-trachytic volcanic geothermal areas, amidst penetration of electromagnetic (EM) waves deep into the subsurface. This is done in an attempt to detect zones with reduced resistivity in the rather highly resistive volcanic area, and thus give information about the prospective geothermal system.

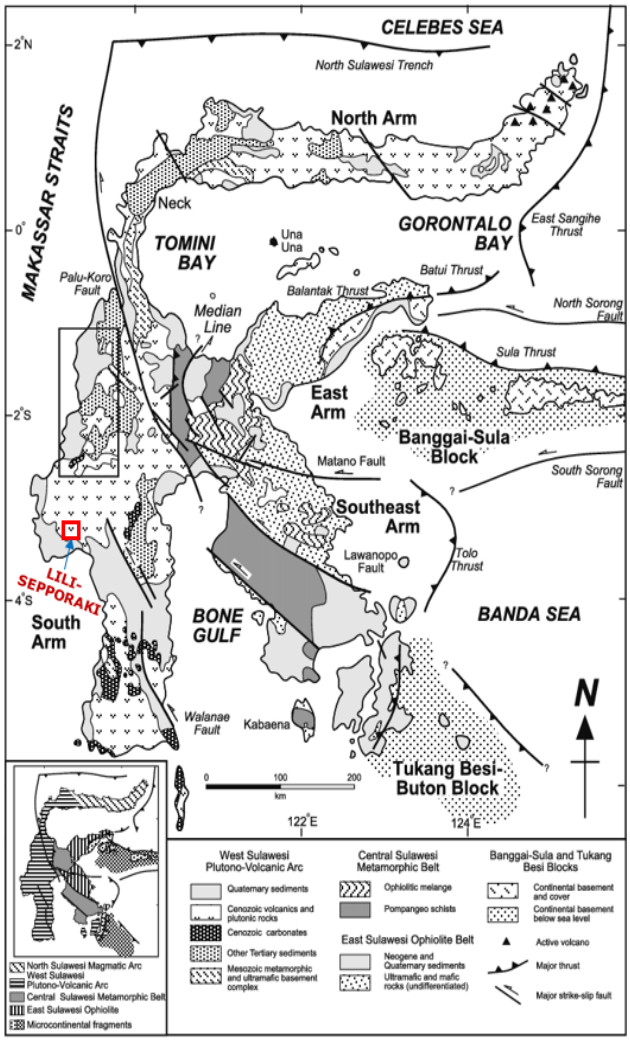

Fig 1: Regional geological map of Sulawesi Showing Lili-Sepporaki Prospect (red square)[13]

Lili geothermal prospect is dominated by andesitic to trachytic volcanic rocks (Fig.1). Volcanic activity is believed to have commenced during the Tertiary era and its products underwent intensive fracturing, to which the permeability worthy to allow passage of hydrothermal fluid, is attributed. Tectonism that occurred during Miocene-Pliocene time allegedly formed the North West-South East (NW-SW) trending faults that serve as conduit for geothermal fluid to the surface [14]. The prospect area has 12 stratigraphic units: [15] Walimbong volcanics (Tvw), Buttu Pakkedong Trachytic lava (Tlp), Inseparable volcanics (Tvt), Buttu Dambu Andesitic lava (Tld), Buttu Talaya Andesitic lava (Tlt), Buttu Sawergading (Tls), and Buttu Kamande Andesitic lava (Tlk) are exposed at the surface and a big chunk of the top layer is weathered, apart from Tvt[13]. Tvt is silicified and composed of spread out structures that are fractured. Formations at near surface such as Porphyry Andesite (Tp), and Tvw hydrothermally altered to form clays such as smectite [16-17]. Formations such as Tlt and Tvw underwent alteration at higher depth to form chlorite minerals [16]. Fractured formations include Tvw, Tp, Tvt, and Feldspathoidal andesite (Tf) while there are structural patterns, some of which contribute to the hot spring discharge [16]. The basement is of metamorphic origin. Geochemical analysis on the hotspring water found out that: the geothermal water has chloride chemistry, using the $Cl\text{-}SO_4\text{-}HCO_3$ trilinear diagram; hot water interacts with the rocks it passes through, to the surface; and hot water interacted with the geothermal system at depth, with reference to both the Na-K-Mg and Cl-Li-B trilinear diagrams [14].

Recent geophysical surveys concluded that the study area is dominated by low magnetic and gravity anomalies in the North, which points to the hydrothermal alteration and weathering of rocks and high gravity and magnetic anomalies in the south [17-20]. 2.5D modelling results from Bouguer anomaly data provide for Tvt as the cap rock, while Tp as the reservoir rock [19].

Temperature gradient drilling data pointed to montmorillonite and palygorskite as the main clay minerals, up to a drilled depth of 700 m [20]

Conductivity, the inverse of resistivity, is a transport property that defines ability of a material to carry an electric current. Conduction in the Earth ensues through the transport of several charge carriers namely: electrons, ions or electron vacancies. Metallic bodies such as chalcopyrite and pyrite are some of the conductors and these are formed through hydrothermal processes at mid-ocean ridges and in continental crust [12]. When subsurface rocks are subjected to compaction, consolidation or diagenesis, their porosity is reduced and thus complicating electrical conduction. Electrical resistivity of rocks is considerably impacted by the shutting down of conduction paths through precipitation and compaction [12]. Several researches attribute the loss of connectivity largely to compaction [21].

For aqueous fluids, resistivity of crustal fluids is mainly determined by concentration of chloride and bicarbonate salt and temperature and fluid density [22]. Crustal fluids particularly hydrothermal brines in volcanic settings at a depth of 8 km or shallower, could have resistivity to a tune of 0.01 Ω m [22-23]. The electrical conductivity of chloride-rich solutions increases almost linearly with temperature, for conductivity values less than 30 S/m [24]. Saline waters can exist at a depth of about 9km with Bavaria- Germany

as an example [25]. Increasing water saturation decreases the resistivity of rocks [26].

Deformed metamorphic rocks usually have strong foliation and this is the reason for the high degrees of electrical anisotropy, more so when carbon is present. Gneisses and granulite can exhibit such anisotropy [27-29]. High-pressure subduction zone eclogites routinely consist of great volume proportions of electrically conductive Fe-rich garnet[30-31]. Garnets could be highly conducting if they are deformed to the point where they intersect, or are linked through metasomatic events.

Clay minerals have resistivity values ranging from 1 – 50 Ohm-m, while igneous and metamorphic rocks are in the range of 500 - 10^7 Ohm-m [32]. Weathered igneous have their resistivities reduced to 2 – 500 Ohm-m [33].

1. Methodology

MT data was collected by the Centre for Minerals, Coal and Geothermal resources (PSDMBP) of the Republic of Indonesia, in 2011 with a station spacing of 1000m to 2000m and the frequency range for recording was 320Hz-0.01Hz. Measurements were carried out from evening through morning with a time lapse between 12-18 hours. Time series data were obtained from the measurement of two components of the electric field (Ex and Ey) and 3 components of the magnetic field (Hx, Hy and Hz) as shown in Fig.2, using Phoenix MTU-5A tool.

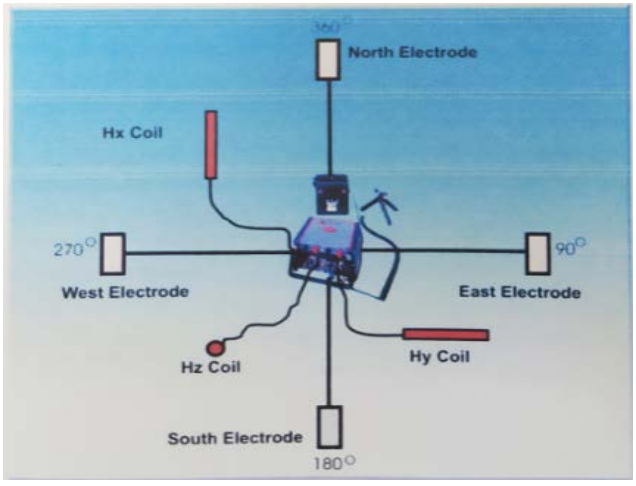

Fig.2: Configuration of electrodes and coils during the Lili-Sepporaki MT survey[8].

The MT method utilizes naturally occurring, broadband electromagnetic waves over the Earth's surface to image subsurface resistivity structure, up to hundreds of kilometers. MT technique measures fluctuations in natural electric (E) and magnetic (B) fields in orthogonal directions at the earth's surface [34]. Solar wind and meteorological activities such as lightening cause natural fluctuations in earth's magnetic field [34-35].

The horizontal E and B fields are related by the impedance tensor [26]. Being a tensor, it also contains information about dimensionality and direction. It is represented by the symbol and expressed in Eq. 1

$$\begin{pmatrix} E_x \\ E_y \end{pmatrix} = \begin{pmatrix} Z_{xx} & Z_{xy} \\ Z_{yx} & Z_{yy} \end{pmatrix} \begin{pmatrix} B_x/\mu_0 \\ B_y/\mu_0 \end{pmatrix} \quad \text{or}$$

$$E = \underline{\underline{Z}} B / \mu_0 \qquad (1)$$

Where: E_x and E_y are the horizontal components of the Electric field; B_x or H_x and B_y or H_y are the horizontal components of the magnetic field; Z_{xx}, Z_{xy}, Z_{yx} *and* Z_{yy} are components of impedance tensor; μ_0 is the magnetic permeability of free space. Impedance is usually expressed in terms of apparent resistivity and phase, and provides information about the subsurface conductivity distribution.

Apparent resistivity is one of the most frequently used parameters for displaying MT data. Apparent resistivity can be defined as the average resistivity of an equivalent uniform half-space of the earth [34]. Apparent resistivity is applied instead of true resistivity for non-uniform earth resistivity, and it depends on the frequency or the period [35]. Impedance (Z) is a complex, being composed of both real and imaginary parts. Therefore, each component of Z has not only a magnitude, but also a phase (φ). Apparent resistivity is defined by Eq.2 and Phase, Eq. 3 [35]

$$\rho_a = 0.2T\left|Z\right|^2 = 0.2T\frac{\left|E\right|^2}{\left|H\right|^2} \qquad (2)$$

$$\varphi = \tan^{-1}\frac{\left(imag.\left[\frac{E_x}{H_y}\right]\right)}{\left(\mathrm{Re}\,al\left[\frac{E_x}{H_y}\right]\right)} \qquad (3)$$

Where E = the horizontal electric field in mv/km, H = the orthogonal horizontal magnetic field in gamma, ρ_a is the apparent resistivity in Ω-m and T is the period in seconds. For a 2D case like this one, resistivity only varies both with depth and along one horizontal direction, and it is constant along the other horizontal direction.

Skin depth, *P(T)*, refers to the penetration depth of Electromagnetic fields into the earth. Extending MT sounding period increases penetration depth as shown in

$(\underline{\underline{Z}})$

eq.4 [36-37]. Frequency is the inverse of Period, *T*, and therefore inversely proportion to skin depth.

$$P(T) \approx 500\sqrt{T\,\rho_a} \qquad (4)$$

SSMT2000 software programme used an input of raw time series files, calibration files, and site parameter files; thus producing Fourier coefficients intermediary; the final output were MT Plot files containing multiple cross-powers for each of the frequencies analysed.

MTEditor programme processed MT Plot files created by SSMT2000; and resistivity and phase curves plus individual cross powers were produced at intermediate stage. Owing to heterogeneity of topography and subsurface conditions, the data had noise and static correction was carried out to remove it. Finally, industry standard EDI files were the final outputs.

Seven representative stations are to be assessed in this study and were chosen from each section of the study area with the Lili Sepporaki hot spring as the reference point.

WinGLink software was used in the production of the resistivity maps that support the MT-plot results. WinGLink involves MT sounding editing, static shifting and MT two-dimensional inversion. In this program, the input are the Industry standard EDI files while resistivity maps are the outputs.

2. Results and Discussion

A sample of seven survey stations were chosen from the five MT lines that were made during the data interpretation (Fig.3).

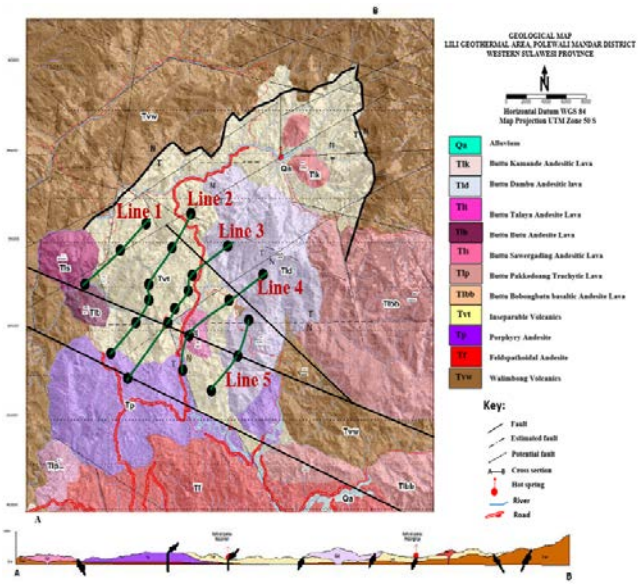

Fig.3: Regional geological map overlain by MT lines (green lines), which are nearly perpendicular to major fault structures (Black lines). Black dots are MT stations[16)]

Resistivity versus frequency MT plots for each of the seven stations are analysed here, in conjunction with the geology of the area.

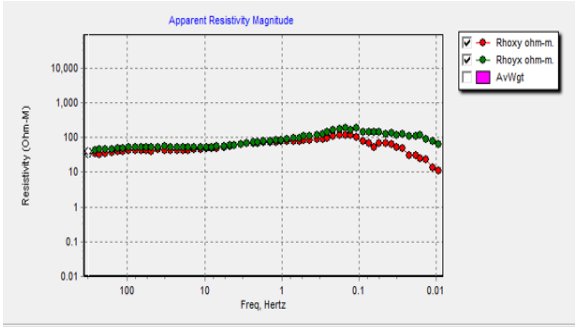

Fig. 4: Resistivity versus frequency for Station MTLL-02. Rhoxy and Rhoyx are almost fused together for most of the displayed frequencies.

Station MTLL-02 (located on Line 1) is located in the western part of the survey area (Fig. 4). Resistivity gradually increases from 50 Ohm-m to 100 Ohm-m between a frequency range of 550Hz to 1 Hz, as EM waves penetrate into the subsurface. This increase in resistivity can be attributed to the increasing depth of penetration of EM waves through the partially weathered rock fromations or the less conductive hydrothermally altered formations such as chlorite. Between 1 Hz and 0.1Hz, the resistivity value slightly goes beyond 100 Ohm-m and this is predicted as change to hot volcanic rocks at depth. Resistivity in the xy direction (Rhoxy) decreases faster than resistivity in yx direction (Rhoyx) for frequencies below 0.1Hz. The reduction in resistivity after 0.2 Hz may be attributed to the presence of saline fluid at depth.

Station MTLL-10 (located on Line 2) is found in the centre of the prospect area (Fig. 5), Northwest of the hot spring. Rhoxy is almost constant until 0.9Hz, it rises sharply between 0.8Hz and 0.2Hz. The rise in Rhoxy is attributed to a transition from highly wethered conductive rocks, through hot volcanic rocks to more resistive, deeper metamorphic rocks . EM waves have higher penetration rate in the yx direction than in the xy direction. Rhoyx gradually rises from 100 Ohm-m to 950 Ohm-m between 20Hz and 0.1Hz. This is so because EM waves penetrate from hot fluid filled rocks to more resistive metamorphic rocks. Resistivity tend to decrease towards 0.01Hz; fractured rocks harboring saline fluids can increase conducitivity. Thus, resistivity decreases.

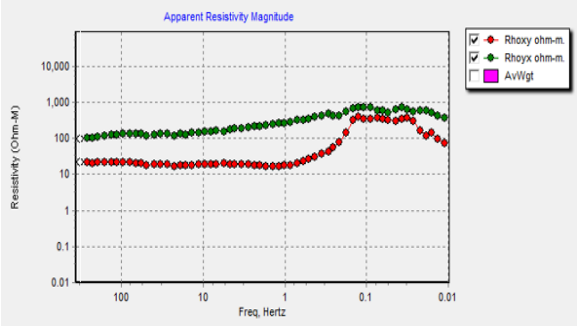

Fig. 5: Resistivity versus frequency for Station MTLL-10. Rhoxy and Rhoyx curves do not meet at all for the displayed frequencies.

Station MTLL-12 (located on Line 2) is situated in the Northern zone of the study area (Fig. 6), north of the hot spring. Rhoxy and Rhoyx take the same trend and similar values between 950Hz and 7Hz. Resistivity decreases between 80 Hz and 8Hz, this is explained by the transition from partially weathered volcanic rocks to more conductive hydothermally altered rocks. The resistivity steadily rises from 0.7Hz to 0.1Hz, attributed to a change through hot fluid-filled rocks and highly resistive basement- geology of the area shows it is a metamorphic rock. Rhoxy experience a decrease as opposed to Rhoyx between 0.08 Hz and 0.01Hz, possibly due to the presence of fluid filled fractures in that direction. The fluids ought to be saline and conductive, hence a decrease in resistvity.

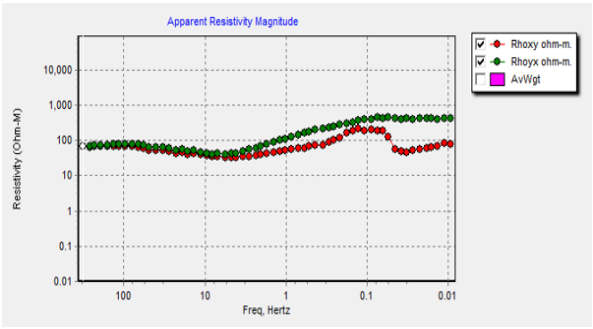

Fig. 6: Resistivity versus frequency for Station MTLL-12

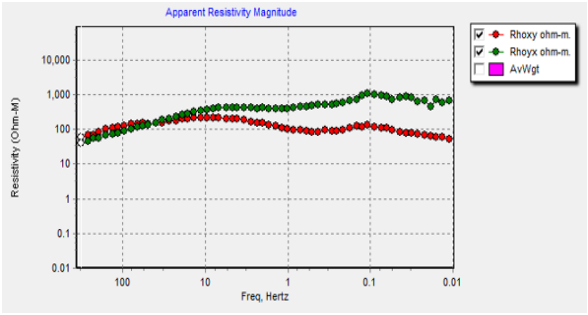

Fig. 7: Resistivity versus frequency for Station MTLL-15A. Rhoyx and Rhoxy meet each other at about 60 Hz.

Station MTLL-15A (Line 3) is hosted in the Southern area of the prospect (Fig. 7), South west of the hot spring. Resistivity in both directions increases between 550Hz and 9Hz, owing to the transition from partially wethered formation through resistive andesitic volcanic rocks, to the more resistive metamorphic rocks. Rhoyx increases further as the EM waves penetrate into more compact basement rocks. At about 8Hz, the trend of Rhoxy and Rhoyx start to change possibly due to a difference in rock properties in the respective directions. Resistivity decreases between 0.1 Hz and 0.01; the possible presence of interconnected fractures that contain conductive saline fluids can be the reason for the decrease.

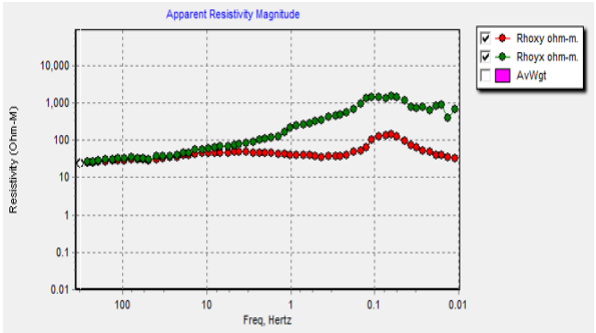

Fig. 8: Resistivity versus frequency for Station MTLL-16A. Rhoyx goes slightly beyong 1,000 Ohm-m.

The hot spring and Station MTLL-16A (located on Line 3) almost share the same spot (Fig. 8). Resistivity in both directions has the same trend from 550Hz to 7Hz. The trend is gradual increase with period and this can accounted for by the change from highly-weathered conductive formations to hydrothermally altered formations. Rhoyx increases sharply between 5Hz and 0.1Hz as the EM waves move through hot fluid-filled volcanic rocks and resistive metamorphic rocks respectively. Resistivity decreases beyond 0.09 Hz and this explained by probably the presence of saline fluids in fractured metamorphic rocks at depth.

The Far Eastern section of the prospect area harbours station MTLL-25 on Line 4 (Fig. 9), North East of the hot spring. Resisitivity in both directions increase between 550hz and 90Hz and then reduces between 90Hz and 9Hz. The trend can be attributed to a transition from highly weathered volcanic rocks, through slightly altered rocks, to more conductive clay-rich formations, respectively. Rhoyx increases sharply after 8Hz because Em waves penetrate from hydrothermally altered formations, through hot fluid-filled volcanic rocks, to highly resistive basement rock.

Almost all the resistvity curves have shown an increase in resistivity beyond 500 Ohm-m as frequency reduces. Formations with the highest resistivity in this survey are the unweathered metamorphic rocks or igneous rocks, and literature has it that their resistivity values range between 500 and 10^7 Ohm-m[32]. As frequency reduces, MT waves penetrate deeper into more compact and consolidated formations- Ionic conduction reduces with increase in compaction and consolidation.

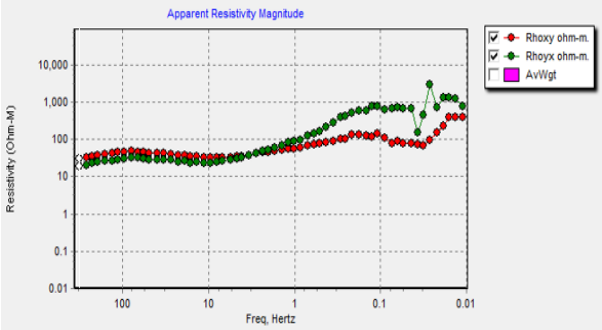

Fig. 9: Resistivity versus frequency for Station MTLL-25. Rhoxy and Rhoyx curves meet each other at 5 Hz.

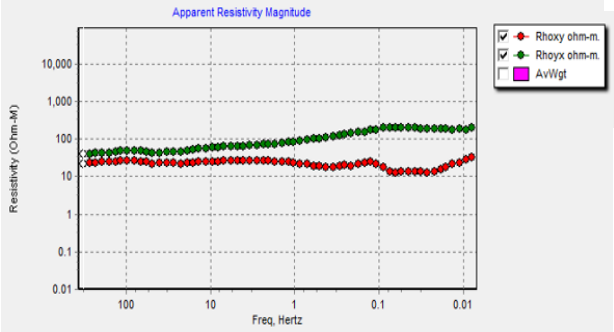

Fig. 10: Resistivity versus frequency for Station MTLL-31. Rhoxy and Rhoyx curves are separated.

The south Eastern zone of the survey area is where Station MTLL-31(Line 5) is located (Fig. 10). EM waves are penetrating faster in the yx direction than in xy. Rhoyx gradually rises between 50Hz and 0.09Hz and Rhoxy is almost constant in this range. This increase in resistivity happens as EM waves penetrate from weathered formations through resistive andesitic rocks**.**

The depth resistivity maps confirm the general increase in resistivity with depth. At a depth of 250 m (Fig. 11), the biggest portion of the map is occupied with a low resistivity anomaly (< 100 Ohm-m). High resistvity only occupies the southern parts of the survey area. At a depth of 750 m (Fig. 12), high resistvity distribution (100 – 250 Ohm-m) spreads further towards the East. Low resistivity anomaly value increases especially in the NE. A very high resistivity anomaly (> 250 Ohm-m) appears for the first time in the South below the hot spring. At 1250 Ohm-m, high resistivity (> 100 Ohm-m) dominates the entire survey area (Fig. 13). Low resistvity (<100 Ohm-m) only appears as smaller portions in the North and East. Generally high resistivity becomes more dominant with depth, as sounding frequency reduces. Fig. 14 shows that the high resistvity anomaly spreads even to the North of the survey area at an elevation of -2250 metres. A low resistivity anoamaly in the west of the survey area can be attributed to the presence of saline fluids in fractured formations. Chlorite-rich alteration products could also account for this anomaly.

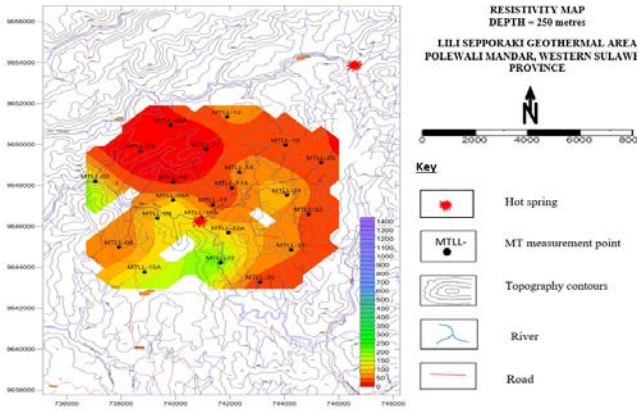

Fig. 11: Resistivity map of Lili-Sepporaki at a depth of 250 m. The map is dominated by low resistivity anomaly (red colour).

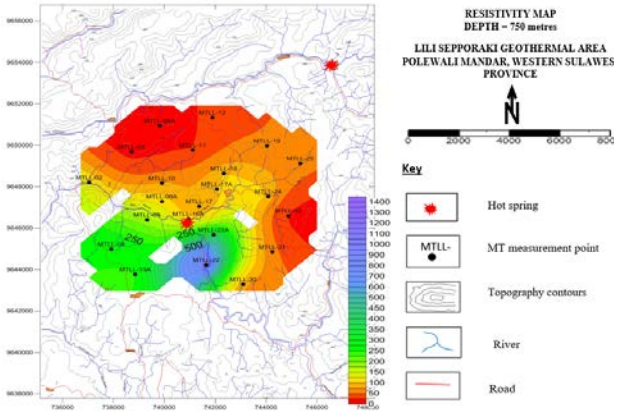

Fig. 12: Resistivity map of Lili-Sepporaki at a depth of 750 m. A very high resistivity anomaly (blue colour) appears below the hot spring.

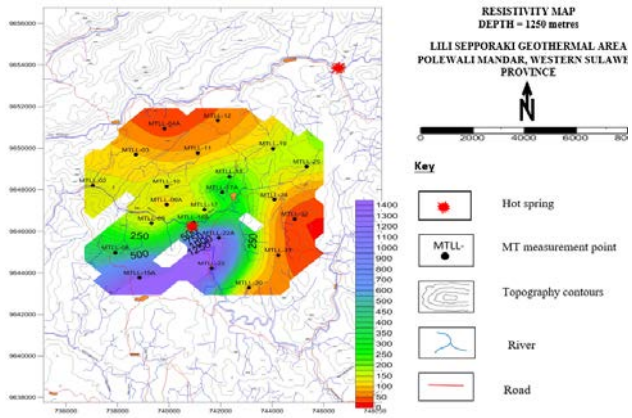

Fig. 13: Resistivity map of Lili-Sepporaki at a depth of 1250 m. High resistivity (yellow, green, blue) dominates the map.

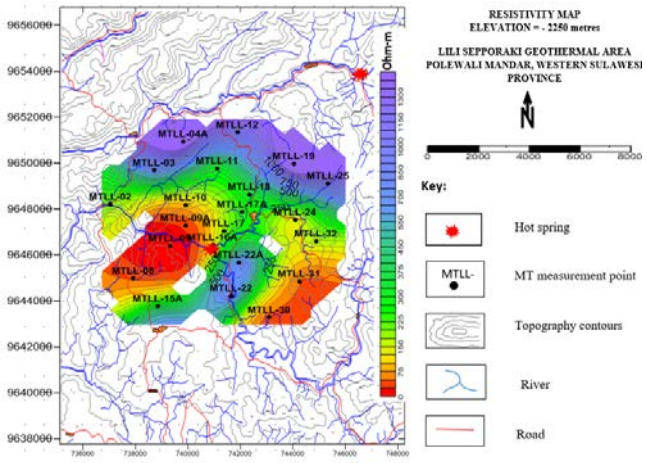

Fig. 14: Resistivity map of Lili-Sepporaki at an elevation of -2250 m. High resistivity anomaly spreads to the North. Low resistivity persists in the West and SE (red).

Geochemistry confirms the existence of a reservoir containing a chloride-rich fluid, as per the $Cl\text{-}SO_4\text{-}HCO_3$ trilinear diagram[14]. This saline fluid (within interconnected pore spaces) has an impact on the bulk resistivity of the rocks which harbours it- the impact is a reduction. Addditionally, the this fluid interacts with the rocks through which it passes, on its way to the surface, thus bringing about alteration of the rocks above the reservoir. Usually alteration products such as clays are minerals are more electrically conductive than the parent rocks. Thus, such affected rocks experience significant reduction in resistvity.

Magnetic and gravity data also support the fact that a big chunk of the surface and near-surface rocks are weathered and hydrothermally altered. Therefore such formations tend to have low restivity anomalies as shown by the MT-plots' findings.

Generally the survey area is under hydrothermal influence because the resistivity values which would be in the tune of 500 to 10^7 Ohm-m for typical igneous and metamorphic rocks, have fallen to less than 500 Ohm-m for the biggest portions of the resistivity curves and maps.

3. Conclusion

Resistivity generally increases with decrease in frequency, that is; less than 100 Ohm-m for frequencies greater than 100 Hz and fluctuates within 100-1000 Ohm-m for frequencies between 1 and 0.1Hz. Frequency is inversely proportional to depth of penetration of the EM waves. Resistivity generally increases with depth. The prospect is defined into three layers depending on the resistivity variation with depth, that is; top-most, middle, and deep. The top-most layer of the prospect area around the hot spring northwards, is covered with weathered and hydrothermally altered and fractured rocks, hence low resistivity; Some areas of the prospect have slightly weathered, less conductive rocks at the surface. Such conductive features are characteristic of impermeable rocks that can work as cap rocks. In other parts the andesitic rocks start from the near-surface downwards. The middle layer is covered with unaltered volcanic rocks filled with hot fluid, which are relatively resistive. Additionally, this layer is composed of fractured or cracked rocks, which are interconnected, and thus the ability to store fluid and act as reservoir. The deep layer is occupied by high resistive rocks and these are mainly metamorphic rocks in this area according to geology; These rocks at depth are most likely fractured and thus have saline fluids. Future research should be directed towards carrying out another MT sounding with more sampling stations, followed by 3D interpretation of data, and exploration drilling in order to understand the geothermal system more, and also get the detailed stratigraphy of the prospect.

Acknowledgement

The authors would like to thank the management of the Centre for Minerals, Coal and Geothermal Resources (PSDMBP) of the Republic of Indonesia, especially the Geophysics department, for the provision of data, regular supervision, and the use of Laboratory facilities.

References

1) B. Prasetyo, Suyanto, M. Oktaufik, S. Himawan, "Design, Construction and Preliminary Test Operation of BPPT-3MW Condensing Turbine Geothermal Power Plant," EVERGREEN Joint Journal of Novel Carbon Resource Sciences & Green Asia Strategy, **06(02)**, 162-167 (2019).
2) A. Fauzi, S. Bahri, and H. Akuanbatin, "Geothermal Development in Indonesia: An Overview of Industry Status and Future Growth," Proceedings World Geothermal Congress 2000, Kyushu - Tohoku, Japan 1109-1114, (2000).
3) H. Akamine, M. Mitsuhara and M. Nishida, "Developments of Coal-Fired Power Plants: Microscopy Study of Fe-Ni Based Heat-Resistant Alloy for Efficiency Improvement," EVERGREEN Joint Journal of Novel Carbon Resource Sciences & Green Asia Strategy, **03(02)**,45-53, (2016).
4) M.S. Abfertiawan, R.S. Gautama, S. B. Kusuma, and S. Notosiswoyo, "Hydrology Simulation of Ukud River in Lati Coal Mine," EVERGREEN Joint Journal of Novel Carbon Resource Sciences & Green Asia Strategy,**03(01)**, pp. 21-31, (2016).
5) R. Yoneda. 2017, "Research and Technical Trend in Nuclear Fusion in Japan," EVERGREEN Joint Journal of Novel Carbon Resource Sciences & Green Asia Strategy, **04(04)**,16-23, (2017).

6) D. A. Wulandari, E. Nasruddin, and Djubaedah, E. Thermal Behavior and Characteristic of Pangandaran Natural Zeolite. EVERGREEN Joint Journal of Novel Carbon Resource Sciences & Green Asia Strategy, **06(03)**, 225-229, (2019).
7) S. Darma, S. Harsoprayitno, B. Setiawan, R. Hadyanto, R.Sukhyar, A.W. Soedibjo, N. Ganefianto, and J. Stimac, "Geothermal Energy Update: Geothermal Energy Development and Utilization in Indonesia," Proceedings World Geothermal Congress 2010 Bali, Indonesia, *1*, (2010).
8) T. S. Magnetotellurik, "Laporan akhir Survei Magnetotelluric Daerah Panas Bumi Lili-Sepporaki," Nomor 10/BP/BGD/2011, pp 2-46, 2011. Pusat Sumber Daya Geologi, Jl. Soekarno Hatta, 444.
9) C. Bromley. Tensor CSAMT study of the fault zone between Waikite and Te Kopia geothermal fields. Journal of geomagnetism and geoelectricity, **45(9),** 887-896, (1993).
10) B. Moskowitz, and D. Norton, "A preliminary analysis of intrinsic fluid and rock resistivity in active hydrothermal systems," Journal of Geophysical Research, **82(36)**, 5787-5795, (1977).
11) J. B. Wright, D. A. Hastings, W. B. Jones, and H. R. Williams, "Geology and mineral resources of West Africa," **187**. London: Allen & Unwin, 1985.
12) A, D. Chave, and A. G. Jones, "The magnetotelluric method: Theory and practice," Cambridge University Press, 2012. ISBN 978-0-521-81927-5 Hardback.
13) R. Hall, and M. E. J. Wilson. Neogene sutures in eastern Indonesia. Journal of Asian Earth Sciences **18(6)**, 781-808, (2000).
14) T. S. Terpadu, "Penyelidikian Panas Bumi Terpadu Geologi, Geokimia dan Geofisika Daerah Panas Bumi Polewali Mandar, Sulawesi Barat," 2010. Pusat Sumber Daya Geologi, Badan Geologi-Kementrian ESDM.
15) M. Kholid, S. Widodo, K. P. B. P. P. Sumber, and D. Geologi, "Survei Magnetotelurik Dan Gaya Berat Daerah Panas Bumi Lilli-Matangnga Kabupaten Polewali Mandar, Provinsi Sulawesi Barat" *1-11*, (2011). Pusat Sumber Daya Geologi, Badan Geologi, JL. Soekarno Hatta, 444.
16) N. D. K. Wicaksono, T. Winarno, and R. K. Ali, "Analisis Karakteristik Alterasi Hidrotermal pada Sumur ND-2 dan Keterkaitannya dengan Sumur ND-1 Dalam Permodelan Sistem Panasbumi Daerah Prospek Panasbumi Lilli-Sepporaki, Kabupaten Polewali Mandar, Provinsi Sulawesi Barat," (2018). Doctoral dissertation, Faculty of Engineering.
17) M. Fitri, L. Hasanah, F.D. E. Latief, and S. Feranie, "The effect of temperature on 3D rock structure of andesite rock sample from potential geothermal area, Sulawesi-Indonesia," In *Journal of Physics: Conference Series* (Vol. **1280**, No. 2, p. 022053). IOP Publishing. (2019, November).
18) J. Sihombing, W. Lestari, and W. Joni, "Subsurface Analysis Using Gravity Data at Lili Sepporaki Geothermal Area," In *IOP Conference Series: Materials Science and Engineering* (Vol. **588**, No. 1, p. 012009). IOP Publishing, (2019, August).
19) A. K. Dewi, "Identifikasi Struktur Dan Model Sistem Panas Bumi Daerah Lilli-Sepporaki Berdasarkan Analisis Data Anomali Bouguer," (2015). PhD diss., Fakultas Teknik.
20) S. Ainul, D. N. Usman, and N. Muhamad, "Aplikasi Metode Horner untuk Menghitung Temperature Gradient Thermal," (2019).
21) W. Zhu, C. David, and T.F. Wong, "Network modeling of permeability evolution during cementation and hot isostatic pressing," J. Geophys. Res., **100**, 15 451–15 464, (1995).
22) B. E. Nesbitt, "Electrical resistivities of crustal fluids," J. Geophys. Res., 98, 4301–4310, (1995).
23) A. Pommier, P. Tarits, S. Hautot, M. Pichavant, B. Scaillet and F. Gaillard, "A new petrological and geophysical investigation of the present-day plumbing system of Mount Vesuvius," Geochem. Geophys. Geosyst., 11, Q07013, (2010c). doi:10.1029/2010GC003059.
24) A. S. Quist, and W. L. Marshall, "Electrical conductances of aqueous sodium chloride solutions from 0 to 800 C and at pressures to 4000 bars," 1968. J. Phys. Chem., **71**, 684–703.
25) E. Huenges, B. Engeser, J. Erzinger, W. Kessels, J. Ku¨ ck, and G. Pusch, "The permeable crust: geohydraulic properties down to 9101 m Depth," J. Geophys. Res. **102**: 18255–18265 (1997).
26) T. Matsui, S. G. Park, M. K. Park, and S. Matsuura, "Relationship between electrical resistivity and physical properties of rocks," In *ISRM International Symposium*. International Society for Rock Mechanics and Rock Engineering, (2000, November).
27) P. W. J. Glover, and F. J. Vine, "Electrical conductivity of carbon-bearing granulite at raised temperatures and pressures," Nature, **360**, 723–726 (1992).
28) M. Lastovickova, G. Losito and A. Trova, "Anisotropy of electrical conductivity of dry and saturated KTB samples," Phys. Earth Planet. Inter., **81**(1–4), 315–324 (1993).
29) K. Fuji-ta, T. Katsura, T. Matsuzaki, M. Ichiki and T. Kobayashi, "Electrical conductivity measurement of gneiss under mid- to lower crustal P–T conditions," 2007. Tectonophysics**, 434**, 93–101.
30) M. Konrad-Schmolke, P. J. O'Brien, C. de Capitani and D. A. Carswell, "Garnet growth at high- and ultra-high-pressure conditions and the effect of element fractionation on mineral modes and composition," Lithos, **103**, 309–332 (2008).
31) C. Romano, B. T. Poe, N. Kreidie and C. A. McCammon, "Electrical conductivities of pyrope–almandine garnets up to 19 GPa and 1700 C," Am. Mineral., **91,** 1371–1377 (2006).

32) "Electrical properties, "https://www.britannica.com/science/rock-geology/Electrical-properties (accessed March 3, 2020).
33) "Electrical conductivity," https://gpg.geosci.xyz/content/physical_properties/physical_properties_conductivity.html (accessed January 29, 2020)
34) F. Simpson, and K. Bahr, "Practical Magnetotellurics," Published by the Press Syndicate of the University of Cambridge," 2005.
35) G. D. Naidu, "Deep Crustal Structure of the Son–Narmada–Tapti Lineament,Central India," Springer Theses, DOI: 10.1007/978-3-642-28442-7_2,_ Springer-Verlag Berlin Heidelberg, 2012.
36) A. N.Tikhonov, "The determination of the electrical properties of deep layers of the Earth's crust," Dokl. Acad. Nauk. SSR **73:** 295–297 (1950).
37) L. Cagniard, "Basic theory of the magnetotelluric method of geophysical prospecting," Geophysics **18:** 605–645 (1953).